Scaling of Anisotropic Flow and Momentum-Space Densities for Light Particles in Intermediate Energy Heavy Ion Collisions

T. Z. Yan[a,b], Y. G. Ma[a] , X. Z. Cai[a], J. G. Chen[a], D. Q. Fang[a], W. Guo[a,b], C. W. Ma[a,b], E. J. Ma[a,b], W. Q. Shen[a], W. D. Tian[a], K. Wang[a,b]

[a] *Shanghai Institute of Applied Physics, Chinese Academy of Sciences, Shanghai 201800, China*
[b] *Graduate School of the Chinese Academy of Sciences, Beijing 100080, China*

Abstract

Anisotropic flows (v_2 and v_4) of light nuclear clusters are studied by Isospin-Dependent Quantum Molecular Dynamics model for the system of $^{86}Kr + ^{124}Sn$ at intermediate energy and large impact parameters. Number-of-nucleon scaling of the elliptic flow (v_2) are demonstrated for the light fragments up to $A = 4$, and the ratio of v_4/v_2^2 shows a constant value of $1/2$. In addition, the momentum-space densities of different clusters are also surveyed as functions of transverse momentum, in-plane transverse momentum and azimuth angle relative to the reaction plane. The results can be essentially described by momentum-space power law. All the above phenomena indicate that there exists a number-of-nucleon scaling for both anisotropic flow and momentum-space densities for light clusters, which can be understood by the coalescence mechanism in nucleonic degree of freedom for the cluster formation.

Anisotropic flow is of interesting subject in theoretical and experimental investigations on nuclear reaction dynamics in intermediate and high energy heavy-ion collisions [1,2,3,4,5,6,7,8,9,10]. Many studies of the dependences of the 1-th and 2-nd anisotropic flows (the directed flow and elliptic flow, respectively) on beam energies, mass number or quark number, isospin and impact parameter revealed much interesting physics about the properties and origin of the collective flow. In particular, recent ultra-relativistic Au + Au collision experiments demonstrated the number of constituent-quark (NCQ) scaling from the transverse momentum dependent elliptic flow for the different mesons and baryons at the Relativistic Heavy Ion Collider (RHIC) in Brookhaven National Laboratory [11], it indicates that the partonic degree of the freedom plays a dominant role in formation of the dense matter in the early stage of collisions. Several theoretical models have been successfully proposed to interpret the NCQ-scaling of hadrons at RHIC [12,13,14,15,16]. In these studies, a popular interpretation is assuming that the mesons and baryons are formed by the coales-

Email address: ygma@sinap.ac.cn.
Corresponding author. (Y. G. Ma[a]).

cence or recombination of the constituent quarks. Moving to the intermediate energy heavy ion collisions, the coalescence mechanism has been also used to explain the formation of light particles and fragments [17,18,19,20,21]. In these studies, however, most observables which one focused on are the spectra of kinetic energy or momentum of light particles. While a few studies investigated the mass dependence of the directed flow [22,23]. Systematic theoretical studies on the flow and momentum space densities of different fragments in intermediate energy domain in terms of the coalescence mechanism are still rare. In this context, we survey, for the first time to our knowledge, the nucleon number dependence of the anisotropic flows v_2 and v_4 in the intermediate energy heavy ion collisions with the coalescence scenario. Moreover, the power law behaviors of light fragment production in momentum space are also explored in our model simulation. Note that this power law behaviors have been experimentally demonstrated in violent collisions at the beam energies between 0.1 A and 15 A GeV [24]. In this Letter we use Isospin-Dependent Molecular Dynamics (IDQMD) model to simulate ^{86}Kr + ^{124}Sn at 25 MeV/nucleon and larger impact parameters (b = 7 - 10 fm), and investigate the outcome of nucleonic coalescence mechanism on the anisotropic flows and momentum space densities of light particle production in intermediate energy heay ion collisions.

Anisotropic flow is defined as the different n-th harmonic coefficient v_n of an azimuthal Fourier expansion of the particle invariant distribution [2]

$$\frac{dN}{d\phi} \propto 1 + 2 \sum_{n=1}^{\infty} v_n cos(n\phi), \qquad (1)$$

where ϕ is the azimuthal angle between the transverse momentum of the particle and the reaction plane. Note that in the coordinate system the z-axis along the beam axis, and the impact parameter axis is labelled as x-axis. The first harmonic coefficient v_1 represents the directed flow, $v_1 = \langle cos\phi \rangle = \langle \frac{p_x}{p_t} \rangle$, where $p_t = \sqrt{p_x^2 + p_y^2}$ is transverse

momentum. v_2 represents the elliptic flow which characterizes the eccentricity of the particle distribution in momentum space,

$$v_2 = \langle cos(2\phi) \rangle = \langle \frac{p_x^2 - p_y^2}{p_t^2} \rangle, \qquad (2)$$

and v_4 represents the 4-th momentum anisotropy,

$$v_4 = \left\langle \frac{p_x^4 - 6p_x^2 p_y^2 + p_y^4}{p_t^4} \right\rangle. \qquad (3)$$

The model we are using in the present work is based on the Quantum Molecular Dynamics (QMD) approach which is an n-body theory to describe heavy ion reactions from intermediate energy to 2 A GeV. It includes several important parts: the initialization of the target and the projectile nucleons, the propagation of nucleons in the effective potential, the collisions between the nucleons, the Pauli blocking effect and the numerical tests. A general review about QMD model can be found in [25]. The IDQMD model is based on QMD model affiliating the isospin factors, which includes the mean field, two-body nucleon-nucleon (NN) collisions and Pauli blocking [26,27,28,29,30].

In the QMD model each nucleon is represented by a Gaussian wave packet with a width $\sqrt{L}$ (here L = 2.16 fm^2) centered around the mean position $\vec{r_i}(t)$ and the mean momentum $\vec{p_i}(t)$,

$$\psi_i(\vec{r}, t) = \frac{1}{(2\pi L)^{3/4}} exp[-\frac{(\vec{r} - \vec{r_i}(t))^2}{4L}]$$

$$exp[-\frac{i\vec{r} \cdot \vec{p_i}(t)}{\hbar}]. \qquad (4)$$

The nucleons interact via nuclear mean field and nucleon-nucleon collision. The nuclear mean field can be parameterized by

$$U(\rho, \tau_z) = \alpha(\frac{\rho}{\rho_0}) + \beta(\frac{\rho}{\rho_0})^{\gamma} + \frac{1}{2}(1 - \tau_z)V_c$$

$$+C_{sym}\frac{(\rho_n - \rho_p)}{\rho_0}\tau_z + U^{Yuk} \qquad (5)$$

with ρ_0 the normal nuclear matter density (here, 0.16 fm^{-3} is used). ρ, ρ_n and ρ_p are the total, neutron and proton densities, respectively. τ_z is zth component of the isospin degree of freedom, which equals 1 or -1 for neutrons or protons, respectively. The coefficients α, β and γ are parameters for nuclear equation of state (EOS). C_{sym} is the symmetry energy strength due to the difference of neutron and proton. In the present work, we take α = -124 MeV, β = 70.5 MeV and γ = 2.0 which corresponds to the so-called hard EOS with an incompressibility of $K = 380$ MeV and $C_{sym} = 32$ MeV [25]. V_c is the Coulomb potential and U^{Yuk} is Yukawa (surface) potential which has the following form:

$$U^{Yuk} = \frac{V_y}{2m}\sum_{i \neq j}\frac{1}{r_{ij}}exp(Lm^2)$$

$$[exp(-mr_{ij})erf(\sqrt{L}m - r_{ij}/\sqrt{4L})$$

$$-exp(mr_{ij})erf(\sqrt{L}m + r_{ij}/\sqrt{4L})] \quad (6)$$

with V_y = 0.0074 GeV, m = 1.25 fm^{-1} and L = 2.16 fm^2. The relative distance $r_{ij} = |\vec{r_i} - \vec{r_j}|$. Experimental in-medium NN cross section parametrization which is energy and isospin dependent is used in this work.

The Pauli blocking effect in IDQMD model is treated separately for the neutron and the proton: whenever a collision occurs, we assume that each nucleon occupies a six-dimensional sphere with a volume of $\hbar^3/2$ in the phase space (considering the spin degree of freedom), and then calculate the phase volume, V, of the scattered nucleons being occupied by the rest nucleons with the same isospin as that of the scattered ones. We then compare $2V/\hbar^3$ with a random number and decide whether the collision is blocked or not.

In the QMD model, the initial momentum of nucleons is generated by means of the local Fermi gas approximation. The local Fermi momentum is given by:

$$P_F^i(\vec{r}) = \hbar(3\pi^2\rho_i(\vec{r}))^{\frac{1}{3}}, (i = n, p). \qquad (7)$$

In the model, the radial density can be written as:

$$\rho(r) = \sum_i \frac{1}{(2\pi L)^{3/2}}exp(-\frac{r^2 + r_i^2}{2L})\frac{L}{2rr_i}$$

$$\times[exp(\frac{rr_i}{L}) - exp(-\frac{rr_i}{L})]. \qquad (8)$$

The time evolution of the colliding system is given by the generalized variational principal. Since the QMD can naturally describe the fluctuation and correlation, we can study the nuclear clusters in the model [25,26,27,28,29,30]. In QMD model, nuclear clusters are usually recognized by a simple coalescence model: i.e. nucleons are considered to be part of a cluster if in the end at least one other nucleon is closer than $r_{min} \leq 3.5$ fm in coordinate space and $p_{min} \leq 300$ MeV/c in momentum space [25]. This mechanism has been extensively applied in transport theory for the cluster formation.

Now we move to the calculations. For an example, we simulated ^{86}Kr + ^{124}Sn at 25 MeV/nucleon and impact parameter of 7 - 10 fm. 50,000 events have been accumulated. The systems tend to freeze-out around 120 fm/c. In this paper, we extract the following physics results at 200 fm/c. The upper panel of Fig. 1 shows transverse momentum dependence of elliptic flows for mid-rapidity light fragments. The range of transverse momentum for different fragments is different according to their masses. From the figure, it shows that the elliptic flow is positive and it increases with the increasing p_t. It reflects that the light clusters are preferentially emitted within the reaction plane, and particles with higher transverse momentum tend to be strongly emitted within in-plane , i.e.

stronger positive elliptic flow. In comparison to the elliptic flow at RHIC energies, the apparent behavior of elliptic flow versus p_t looks similar, but the mechanism is obviously different. In intermediate energy domain, collective rotation is one of the main mechanisms to induce the positive elliptic flow [31,32,33,34,35,36]. In this case, the elliptic flow is mainly driven by the attractive mean field. However, the strong pressure which is built in early initial geometrical almond-type anisotropy due to the overlap zone between both colliding nuclei in coordinate space will rapidly transforms into the azimuthal anisotropy in momentum space at RHIC energies [11]. In other words, the elliptic flow is mainly driven by the stronger outward pressure. The lower panel displays the elliptic flow per nucleon as a function of transverse momentum per nucleon, and it looks that there exists the number of nucleon scaling when $p_t/A < 0.25$ GeV/c. This behavior is apparently similar to the number of constituent quarks scaling of elliptic flow versus transverse momentum per constituent quark (p_t/n) for mesons and baryons which was observed at RHIC [11].

The RHIC experimental data demonstrated a scaling relationship between 2-nd flow (v_2) and n-th flow (v_n), namely $v_n(p_t) \sim v_2^{n/2}(p_t)$ [37]. It has been shown [38,39] that such scaling relation follows from a naive quark coalescence model [13] that only allows quarks with equal momentum to form a hadron. Denoting the meson anisotropic flows by $v_{n,M}(p_t)$ and baryon anisotropic flows by $v_{n,B}(p_t)$, Kolb et al. found that $v_{4,M}(p_t) = (1/4)v_{2,M}^2(p_t)$ for mesons and $v_{4,B}(p_t) = (1/3)v_{2,B}^2(p_t)$ for baryons if quarks have no higher-order anisotropic flows. Since mesons dominate the yield of charged particles in RHIC experimental data, the smaller scaling factor of 1/4 than the empirical value of about 1 indicates that higher-order quark anisotropic flows cannot be neglected. Including the latter contribution, one can show that

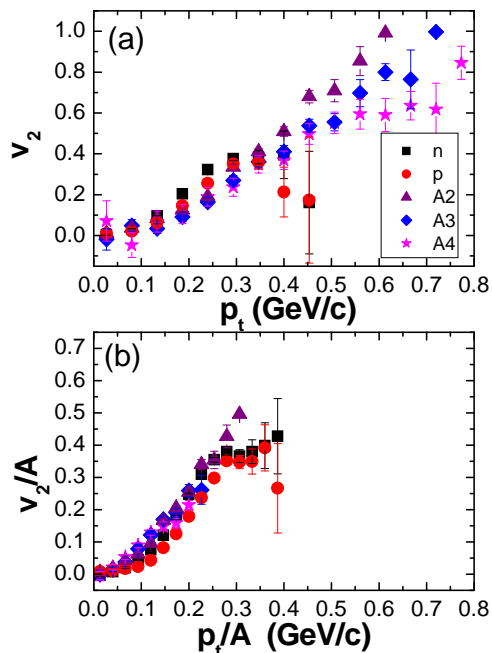$$\frac{v_{4,M}}{v_{2,M}^2} \approx \frac{1}{4} + \frac{1}{2}\frac{v_{4,q}}{v_{2,q}^2}, \qquad (9)$$

Fig. 1. (a) Elliptic flow as a function of transverse momentum (p_t). Squares represent for neutrons, circles for protons, triangles for fragments of $A = 2$, diamonds for $A = 3$ and stars for $A = 4$; (b) Elliptic flow per nucleon as a function of transverse momentum per nucleon. The symbols are the same as (a).

and

$$\frac{v_{4,B}}{v_{2,B}^2} \approx \frac{1}{3} + \frac{1}{3}\frac{v_{4,q}}{v_{2,q}^2}, \qquad (10)$$

where $v_{n,q}$ denotes the quark anisotropic flows. The meson anisotropic flows thus satisfy the scaling relations if the quark anisotropic flows also satisfy such relations. However, this ratio is experimentally determined to be 1.2 [40], which means that the fourth-harmonic flow of quarks v_4^q must be greater than zero. One can go one step further and assume that the observed scaling of the hadronic v_2 actually results from a similar scaling occurring at the partonic level. In this case $v_4^q = (v_2^q)^2$ and the hadronic ratio v_4/v_2^2 then equals $1/4+1/2 = 3/4$ for mesons and $1/3 + 1/3 = 2/3$ for baryons, respectively. Again, since this value is measured to be 1.2, even the partonic v_4^q must be greater than simple scaling and quark coalescence models predict.

4

Recognizing the above behaviors of the flows at RHIC energies, we would like to know what the higher order momentum anisotropy in the intermediate energy is. So far, there is neither experimental data nor theoretical investigation for the higher order flow, such as v_4, in this energy domain. In the present work, we explore the behavior of v_4 in the model calculation. Fig. 2 shows the feature of v_4. Similar to the relationship of v_2/A versus p_t/A, we plot v_4/A as a function of p_t/A. The divergence of the different curves between different particles in Fig. 2(a) indicates no simple scaling of nucleon number for 4-th momentum anisotropy. However, if we plot v_4/A^2 versus $(p_t/A)^2$, it looks that the points of different particles nearly merge together and it means a certain of scaling holds between two variables. Due to a nearly constant value of v_4/v_2^2 in the studied p_t range (see Fig. 2(c)) together with the number-of-nucleon scaling behavior of v_2/A vs p_t/A, v_4/A^2 should scale with $(p_t/A)^2$, as shown in Fig. 2(b). If we assume the scaling laws of mesons (Eq.(9)) and baryons (Eq.(10)) are also valid for A = 2 and 3 nuclear clusters, respectively, then v_4/v_2^2 for A = 2 and 3 clusters indeed give the same value of $1/2$ as nucleons, as shown in Fig. 2(c). Coincidentally the predicted value of the ratio of v_4/v_2^2 for hadrons is also $1/2$ if the matter produced in ultra-relativistic heavy ion collisions reaches to thermal equilibrium and its subsequent evolution follows the laws of ideal fluid dynamics [41]. It is interesting to note the same ratio was predicted in two different models at very different energies, which is of course worth to be further investigated in near future. Overall speaking, we learn that v_4/v_2^2 is approximately $1/2$ in nucleonic level coalescence mechanism, which is different from $3/4$ for mesons or $2/3$ for baryons in partonic level coalescence mechanism.

Measurements of inclusive single-particle spectra from heavy-ion collisions indicate a simple empirical pattern of light fragment production: the observed invariant momentum-space density ρ_A for fragments with mass number A closely follows the A-th power of the observed proton density
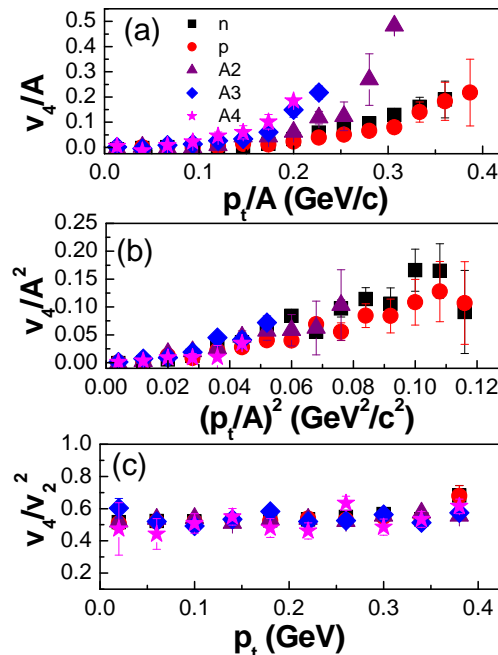

Fig. 2. (a) v_4/A as a function of p_t/A for different particles, namely, neutrons (squares), protons (circles), fragments of $A = 2$ (triangles), $A = 3$ (diamonds) and $A = 4$ (stars). (b) v_4/A^2 as a function of $(p_t/A)^2$. (c) the ratios of v_4/v_2^2 for different particles vs p_t.

ρ_1^A. It was shown that this power law behavior is valid for spectra of participant fragments up to $A = 14$ with projectiles ranging from protons to Au at a variety of beam energies between 0.1 A and 15 A GeV [24]. However, there are rare experimental data and calculations to test the power law at intermediate energies. In the present work, we test the momentum-space power law up to $A = 4$ by IDQMD.

The upper panels of Fig. 3 show the transverse momentum space densities $\rho = A^2 dN/p_t dp_t$. The results also show a level of adherence to power law behavior at high p_t/A, which is similar to what have been previously reported for single-particle-inclusive measurements [42], and reflects the persistence of momentum-space coalescence behavior for intermediate energy ^{86}Kr + ^{124}Sn collisions. The middle panels of Fig. 3 depict the density in the in-plane transverse momentum
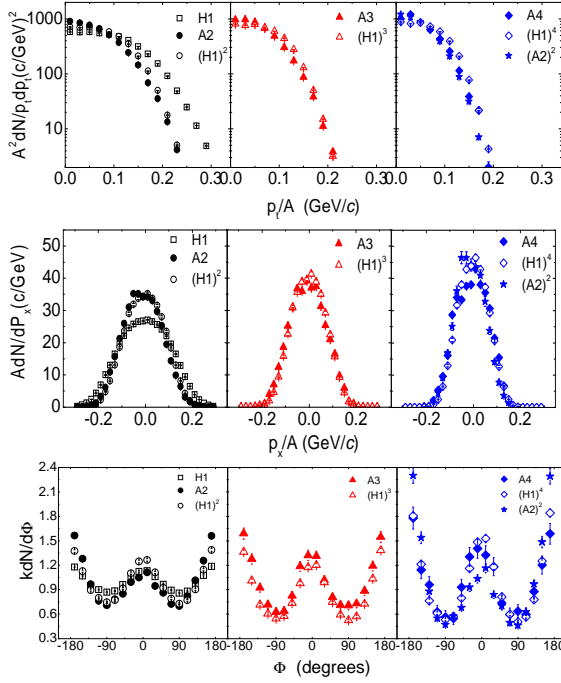
Fig. 3. Upper panels: transverse momentum-space density for light fragments; Middle panels: in-plane transverse momentum space density; Bottom panels: azimuthal distributions relative to the reaction plane. The open squares represent the density for protons, the solid circles for the fragments with $A = 2$, the open circles for the proton density squared normalized to the same area as the proton density, the solid triangles for $A = 3$, the open triangles for protons to the power of 3, the solid diamonds for $A = 4$, the open diamonds for protons to the power of 4, and the stars for the $A = 2$ density squared.

space (p_x/A). The densities are also normalized to the same area as the proton density. Wang *et al.* first introduced the momentum-space power law to $\rho(p_x)$ [42]. Again, our results show a level of adherence to power law behavior. The bottom panels of Fig. 3 depicts the azimuthal (ϕ) distribution of fragments relative to the reaction plane. The factor k is chosen so that the mean values of $dN/d\phi$ are fixed to be 1. Essentially the power-law behavior remains for the azimuthal distributions of these light fragments. From all the above distributions, nucleon coalescence mechanism keeps valid in the momentum space densities.

In summary, we applied IDQMD model to investigate the behavior of anisotropic flows, namely v_2 and v_4, versus transverse momentum for the light fragments from 25 MeV/nucleon ^{86}Kr + ^{124}Sn collisions at 7-10 fm of impact parameters. Both v_2 and v_4 generally show positive values and increase with p_t. By the number-of-nucleon scaling, the curves of elliptic flow for different fragments approximately collapse on the similar curve, which means that there exists an elliptic flow scaling on the nucleon number for light fragments. This phenomenon is similar to the NCQ scaling of elliptic flows of hadrons at RHIC energies where elliptic flow can be developed in the early partonic stage of collisions, but here it is a nucleonic level in intermediate energy collisions. For 4-th momentum anisotropy v_4, it seems to be scaled by v_2^2 and $v_4/v_2^2 \sim 0.5$. It will be of very interesting if one can measure this ratio in intermediate energy HIC. In addition, we also investigated momentum-space densities of light fragments as functions of fragment transverse momentum p_t, in-plane transverse momentum p_x and the azimuth angle relative to the reaction plane. All these observables are well described by the momentum-space power law which has been well experimentally observed at high energies. All the above phenomena can be seen as an outcome of the nucleonic coalescence which results that the number-of-nucleon scaling of both flow and momentum space density in intermediate energy heavy ion collision. It may indicate that nucleonic matter may be one of the middle transit stage before chemical freeze-out takes place.

References

[1] J. Ollitrault, Phys. Rev. D 46 (1992) 229.

[2] S. Voloshin, Y. Zhang, Z. Phys. C 70 (1996) 665.

[3] H. Sorge, Phys. Lett. B 402 (1997) 251; Phys. Rev. Lett. 78 (1997) 2309 ; 82 (1999) 2048.

[4] P. Danielewicz, R. A. Lacey, P. B. Gossiaux et al., Phys. Rev. Lett. 81 (1998) 2438.

[5] B. Zhang, M. Gyulassy, and C. M. Ko, Phys. Lett. B 455(1999) 45.

[6] D. Teaney and E. V. Shuryak, Phys. Rev. Lett. 83 (1999) 4951.

[7] P. F. Kolb, J. Sollfrank, and U. Heinz, Phys. Rev. C 62 (2000) 054909.

[8] Y. Zheng, C. M. Ko, B. A. Li, and B. Zhang, Phys. Rev. Lett. 83 (1999) 2534.

[9] D. Perslam and C. Gale, Phys. Rev. C 65 (2002) 064611.

[10] J. Lukasik et al. (INDRA-ALDAIN Collaboration), Phys. Lett. B 608 (2004) 223.

[11] J. Adams et al., Phys. Rev. Lett. 92 (2004) 052302; Phys. Rev. C 72 (2005) 014904; Phys. Rev. Lett. 95 (2005) 122301;

[12] Zi-Wei Lin and C. M. Ko, Phys. Rev. Lett. 89 (2002) 202302; V. Greco, C. M. Ko, and P. Lévai, Phys. Rev. C 68 (2003) 034904 .

[13] D. Molnár and S. A. Voloshin, Phys. Rev. Lett. 91 (2003) 092301.

[14] R. J. Fries, B. Müller, C. Nonaka, and S. A. Bass, Phys. Rev. Lett. 90 (2003) 202303; Phys. Rev. C 68 (2003) 044902.

[15] R. C. Hwa and C. B. Yang, Phys. Rev. C 66 (2002) 025205; Phys. Rev. C 70 (2004) 024904.

[16] J. H. Chen, Y. G, Ma, G. L. Ma et al., arXiv:nucl-th/0504055.

[17] T. C. Awes, G. Poggi, C. K. Gelbke et al., Phys. Rev. C 24 (1981) 89.

[18] A. Z. Mekjian, Phys. Rev. C 17 (1978) 1051; Phys. Rev. Lett. 38 (1977) 640; Phys. Lett. 89B (1980) 177 .

[19] H. Sato and K. Yazaki, Phys. Lett. 98B (1981) 153.

[20] W. J. Llope, S. E. Pratt, N. Frazier et al., Phys. Rev. C 52 (1995) 002004.

[21] K. Hagel, R. Wada, J. Cibor et al., Phys. Rev. C 62 (2000) 034607.

[22] M. J. Huang, R. C. Lemmon, F. Daffin, et al., Phys. Rev. Lett. 77(1996) 3739 .

[23] G. J. Kunde, W. C. Hsi, W. D. Kunze et al., Phys. Rev. Lett. 74 (1995) 38.

[24] H. H. Gutbrod et al., Phys. Rev. Lett. 37 (1976) 667; M. C. Lemaire et al., Phys. Lett. 85B (1979) 38; B. V. Jacak, D. Fox, and G. D. Westfall, Phys. Rev. C 31 (1985) 704; S. Hayashi et al., Phys. Rev. C 38 (1988) 1229; N. Saito et al., Phys. Rev. C 49 (1994) 3211; J. Barette et al., Phys. Rev. C 50 (1994) 1077; Z. Phys. C 70 (1996) 665.

[25] J. Aichelin, Phys. Rep. 202 (1991) 233.

[26] Y. G. Ma and W.Q. Shen, Phys. Rev. C 51 (1995) 710.

[27] J.Y. Liu, Y.F. Yang, W. Zuo et al., Phys. Rev. C 63 (2001) 54612.

[28] Y. B. Wei, Y. G. Ma, W. Q. Shen et al., Phys. Lett. B 586 (2004) 225; J. Phys. G 30 (2004) 2019.

[29] Y. G. Ma, H. Y. Zhang and W. Q. Shen, Prog. Phys. (in Chinese) 22 (2002) 99.

[30] Y. G. Ma, Y. B. Wei, W. Q. Shen et al., Phys. Rev. C 73 (2006) 014604.

[31] For a review, see W. Reisdorf and H. G. Ritter, Annu. Rev. Nucl. Part. Sci. 47 (1997) 663.

[32] J. P. Sullivan and J. Péter, Nucl. Phys. A 540 (1992) 275.

[33] W. Q. Shen, J. Péter, G. Bizard et al., Nucl. Phys. A 551 (1993) 333.

[34] Y. G. Ma et al., Phys. Rev. C48 (1993) R1492; Z. Phys. A 344 (1993) 469; Phys. Rev. C51 (1995) 1029; Phys. Rev. C 51 (1995) 3256.

[35] R. Lacey, A. Elmaani, J. Lauret et al., Phys. Rev. Lett. 70 (1993) 1224.

[36] Z. Y. He, J.C. Angelique, A. Auger et al., Nucl. Phys. A 598 (1996) 248.

[37] J. Adams et al. [STAR Collaboration], Phys. Rev. Lett. 92 (2004) 062301.

[38] P. F. Kolb, L. W. Chen, V. Greco, C. M. Ko, Phys. Rev. C69 (2004) 051901.

[39] L. W. Chen, C. M. Ko, Zi-Wei Lin, Phys. Rev. C69 (2004) 031901.

[40] M. D. Oldenburg [STAR Collaboration], nucl-ex/0412001, J. Phys. G 31 (2005) S437.

[41] N. Borghini and J-Y. Ollitrault, nucl-th/0506045.

[42] S. Wang, S. Albergo, F. Bieser et al., Phys. Rev. Lett. 74 (1995) 2646.